Submitted to

31st International Conference on High Energy Physics, ICHEP02, July 24, 2002, Amsterdam
Abstract: **1000**
Parallel Session **5, 6**

www-h1.desy.de/h1/www/publications/conf/conf_list.html

Forward π^0 Production in DIS at HERA

H1 Collaboration

Abstract

The dynamics of QCD evolution at low values of Bjorken-x is studied via the measurement of hard π^0 probes in deeply inelastic positron proton scattering with the H1 experiment. The π^0 mesons are measured in a region of small angles with respect to the proton remnant in the laboratory frame, the so-called forward region.
Differential cross sections for inclusive π^0-meson production are presented as a function of Bjorken-x and π^0 transverse momentum, in different regions of the four momentum transfer Q^2. The accompanying transverse energy flow around the π^0 is also studied. The data are used to discriminate between different QCD evolution schemes for the parton ladder between proton and photon.

1 Introduction

The HERA collider has extended the available kinematic space for Deep-Inelastic Scattering (DIS) to regions of large values of the four momentum transfer Q^2 ($\leq 10^5\ GeV^2$) and small Bjorken-x ($x \approx 10^{-5}$). A variety of measured processes has made detailed tests of perturbative QCD possible. In particular, studies at low x could reveal novel features of parton dynamics. At small x it is very probable that the quark struck by the virtual photon originates from a QCD cascade initiated by a parton in the proton. In different regions of the Q^2 and x different schemes are expected to describe the parton evolution: the mostly discussed being DGLAP[1], BFKL[2] and CCFM[3]. At high Q^2 and high x the initial state radiation is described by the conventional DGLAP evolution equations which resum the leading $\alpha_s \ln(Q^2/Q_\circ^2)$ terms. In this scheme a space-like chain of subsequent gluon emissions is characterized by a strong ordering in transverse momenta k_T. However, at small x the contribution of large $\ln(1/x)$ terms may become important. Resummation of these terms leads to the BFKL evolution equation. No ordering on transverse momenta k_T of emitted gluons is imposed here. The CCFM evolution equation based on angular ordering and colour coherence interpolates between the BFKL and DGLAP approaches.

An extended parton ladder at low x leads to high k_T partonic emission in the forward region to which measurements of jets and leading particles are sensitive. Production of DIS events with a single forward particle is a more refined version of forward jet production: a forward parton is tagged by its single energetic fragmentation product. In analogy to the forward jet analysis, inspired by the proposal of Mueller[4], selection of a single particle with transverse momentum squared ${k_T}^2$ of the order of Q^2, ${k_T}^2 \approx Q^2$, suppresses the k_T ordered DGLAP evolution and the choice of the fractional momentum $x_\pi = E_\pi/E_p$ (E_p is the proton beam energy) greater than Bjorken-x enhances the phase space for BFKL effects. An advantage of studying single particles as opposed to jets is the potential to reach smaller angles, closer to the initial proton direction, than is possible with jets which have a broad spatial extension. A disadvantage is that the cross section of the process is suppressed in comparison to forward jet production, and that fragmentation effects are more significant.

Differential cross-sections for inclusive π^0-meson production[5] have recently been measured by the H1 Collaboration. A BFKL calculation incorporating some of the NLO effects [6] was found to be in good agreement with the data, although the absolute normalization remained strongly affected by the scale uncertainty. A reasonable description of the data is also achieved in the Monte Carlo model RAPGAP[7], based on the DGLAP formalism with inclusion of resolved photon processes.

In this analysis we present new results on high transverse momentum forward π^0 production in DIS with a statistically increased (by a factor 3.5) sample that allows for more differential studies. Additional characteristics of the hadronic final are also studied.

2 Experimental setup and data selection

The data used for this analysis were collected in 1996 and 1997 with the H1 detector at HERA, in collisions of positrons and protons with energies of 27.5 GeV and 820 Gev, respectively. The data correspond to an integrated luminosity of 21 pb^{-1}. A detailed description of the

H1 detector can be found elsewhere[8]. DIS events are selected by identification of scattered positrons in the backward lead/scintillating fiber calorimeter, which has an energy resolution of $\sigma_E/E \approx 0.075/\sqrt{E}$ for electrons. The analysis is restricted to the kinematical range $0.1 < y < 0.6$, $2.0 < Q^2 < 70.0$ GeV^2, and Bjorken-x extends over two orders of magnitude down to $x \approx 10^{-5}$. In this kinematical region the background from photoproduction is negligible.
The π^0-mesons are measured in the finely segmented liquid argon (LAr) calorimeter consisting of an electromagnetic section, that provides an energy resolution of $\sigma_E/E \approx 0.12/\sqrt{E}$, and of a hadronic section which has an energy resolution for charged pions of $\sigma_E/E \approx 0.50/\sqrt{E}$. The absolute energy scales are known to $\pm$ 3% for electromagnetic showers in the forward region relevant to this analysis, and to $\pm$ 4% for hadrons as measured in test beams.
The π^0-mesons are identified via the dominant decay channel $\pi^0 \rightarrow 2\gamma$ using calorimetric information only. The π^0 candidates are selected in the HERA laboratory frame [1] with polar angles in the region $5^\circ < \Theta_\pi < 25^\circ$ and with x_π greater than 0.01. The cut on the minimum transverse momentum of the π^0-meson, $p^*_{T,\pi}$ defined in the photon-proton center of mass system (CMS) is set to 2.5 GeV. For the high π^0 energies requested here, the decay photons cannot be separated in the LAr calorimeter and their energy deposits are reconstructed as one calorimetric cluster. Photon induced showers are selected following a detailed analysis of longitudinal and transverse shower shape development in the LAr calorimeter as described in[5]. The efficiency for finding π^0-mesons after all selection cuts is above 45% and the purity of the selected π^0-meson sample is about 80%. In the selected kinematical range about 5500 (2000) π^0 candidates are found with $p^*_{T,\pi} > 2.5(3.5)$ GeV. Other sources of high energy photons (such as prompt photon production) are negligible[9]. The small contribution of η-meson production is corrected for using Monte Carlo models LEPTO[10] and ARIADNE[11].

3 Results

Inclusive forward π^0 cross-sections for $p^*_{T,\pi} >$ 2.5 GeV and $p^*_{T,\pi} >$ 3.5 GeV are shown as a function of x for different regions of Q^2 in Fig.1 and Fig.2, respectively . All cross-sections are corrected for detector effects and for the influence of QED radiation by a bin-by-bin unfolding procedure, using two Monte Carlo models LEPTO and ARIADNE. Systematic errors are dominated by the model dependence of these corrections which gives rise to typically 10-15 % uncertainty.
In the following, the data are compared with predictions of the Monte Carlo models RAPGAP[7] and CASCADE[12]. RAPGAP implements a QCD model based on LO DGLAP parton showers with (DIR+RES in the figures) and without (DIR in the figures) resolved photon processes. The RAPGAP calculations were made with the CTEQ4M[13] parton densities for the proton and with the GRV[14] parton densities for the virtual photon. CASCADE has been used as an implementation of the CCFM equation.
The prediction of RAPGAP with a point-like photon is well below the data. A reasonable description of the cross-sections is obtained by including in RAPGAP an additional resolved photon contribution and using a renormalisation and factorisation scale of $Q^2 + 4p_T^2$. CASCADE undershoots the data for lower values of Q^2.
The π^0 cross-section as a function of the π^0 transverse momentum $p^*_{T,\pi}$, in the photon-proton

[1]H1 uses a a right-handed coordinate system with the z-axis defined by the incident proton beam.

CMS, is presented in Fig.3 for different regions of Q^2. The measurements extend to values of $p^*_{T,\pi}$ of about 15 GeV and, again, are best described by RAPGAP with a renormalisation and factorisation scale set to $Q^2 + 4p_T^2$.
Fig.4 shows the transverse energy flow around the forward π^0 in the photon-proton CMS, for different ranges of the π^0 pseudorapidity η^*_π, as a function of the distance from the π^0 direction in units of pseudorapidity. Energies deposited at the polar angle $\Theta > 4°$, limited by the acceptance of the LAr calorimeter, are counted here. The energy flow is highly collimated around the direction of the π^0. The π^0 itself contributes , on average, about 4 GeV of transverse energy in the bin containing this particle. Large amounts of transverse energy are also produced away from the π^0. The QCD models presented here give similar predictions. However, the calculations which include resolved processes tend to agree better with the data.
The transverse energy flow around the π^0 reflects how the transverse momentum of the jet is compensated along the ladder. It is best seen in the E_T flow distribution for the most forward π^0's shown in the left upper plot of Fig.4. RAPGAP with direct photon contribution only predicts less radiation in the vicinity of the π^0. The transverse momentum of the forward particle is mainly compensated far away from the π^0, as expected for k_T ordered DGLAP emissions. In the CCFM approach, there is more QCD radiation close to the π^0 direction. The prediction of RAPGAP with a resolved γ^* component lies between predictions of CASCADE and RAPGAP-DIR.
The mean transverse energy along the ladder, in the region $0.5 < \eta^* - \eta^*_\pi < 3.0$, for different ranges of η^*_π in the hadronic CMS as a function of Bjorken x is presented in Fig.5. The data show, within errors, no dependence on x and are best described by RAPGAP with resolved photon interactions.

4 Summary

New measurements of the forward π^0 cross-sections and their accompanying energy flow were presented. The data discriminate between different QCD models and are best described by an approach in which the partonic substructure of virtual photons is taken into account. The fact that CASCADE describes the forward jet cross-section[15] but not the forward π^0 production may indicate the importance of the quark splitting functions which are not taken into account in CASCADE.

References

[1] V.N. Gribov,L.N. Lipatov, Sov.J.Nucl.Phys. 15 (1972) 438 and 675;
Yu. L. Dokshitzer, Sov. Phys. JETP 46 (1977) 641;
G. Altarelli,G. Parisi, Nucl. Phys. 126 (1978) 297.

[2] E.A. Kuraev, L.N. Lipatov, V.S. Fadin, Sov. Phys. JETP 45 (1972) 199;
Y.Y. Balitsky, L.N. Lipatov, Sov.J.Nucl. Phys. 28 (1978) 822.

[3] M. Ciafaloni, Nucl. Phys. B 296 (1988) 49;
S. Catani, F. Fiorani, G. Marchesini, Phys. Lett B234 (1990) 339;

S. Catani, F. Fiorani, G. Marchesini, Nucl. Phys. B 336 (1990) 18;
G. Marchesini, Nucl. Phys. B 445 (1995) 49.

[4] A.H. Mueller, Nucl. Phys. B (Proc. Suppl.) 18 C (1990) 125;
J. Phys. G 17 (1991) 1443;

[5] H1 Collaboration, C. Adloff *et al.*, Phys. Lett B 462 (1999) 440.

[6] J. Kwiecinski, A. Martin, J. Outhwaite, Eur. Phys. J. C9 (1999) 611.

[7] H. Jung, Comp. Phys. Comm. 86 (1995) 147.

[8] H1 Collaboration., I. Abt *et al.*, Nucl. Instr. and Meth. A 386 (1997) 310;348

[9] J. Kwiecinski, S.C. Lang, A.D. Martin, Phys. Rev. D 55 (1997) 1273.

[10] G. Ingelman, A. Edin and J. Rathsman, Comp. Phys. Comm. 101 (1997) 108.

[11] L. Lőnnblad, Comp. Phys. Comm. 71 (1992) 15.

[12] H. Jung, Comp. Phys. Com. 143 (2002) 100.

[13] CTEQ Collab., H.L. Lai et al., Phus.Rev. D 55 (1997) 1280.

[14] M. Glűck, E. Reya and A. Vogt, Phys.Rev. D 46 (1992) 1973;

[15] H. Jung, G.P. Salam, Eur. Phys. J. C 19 (2001) 351.

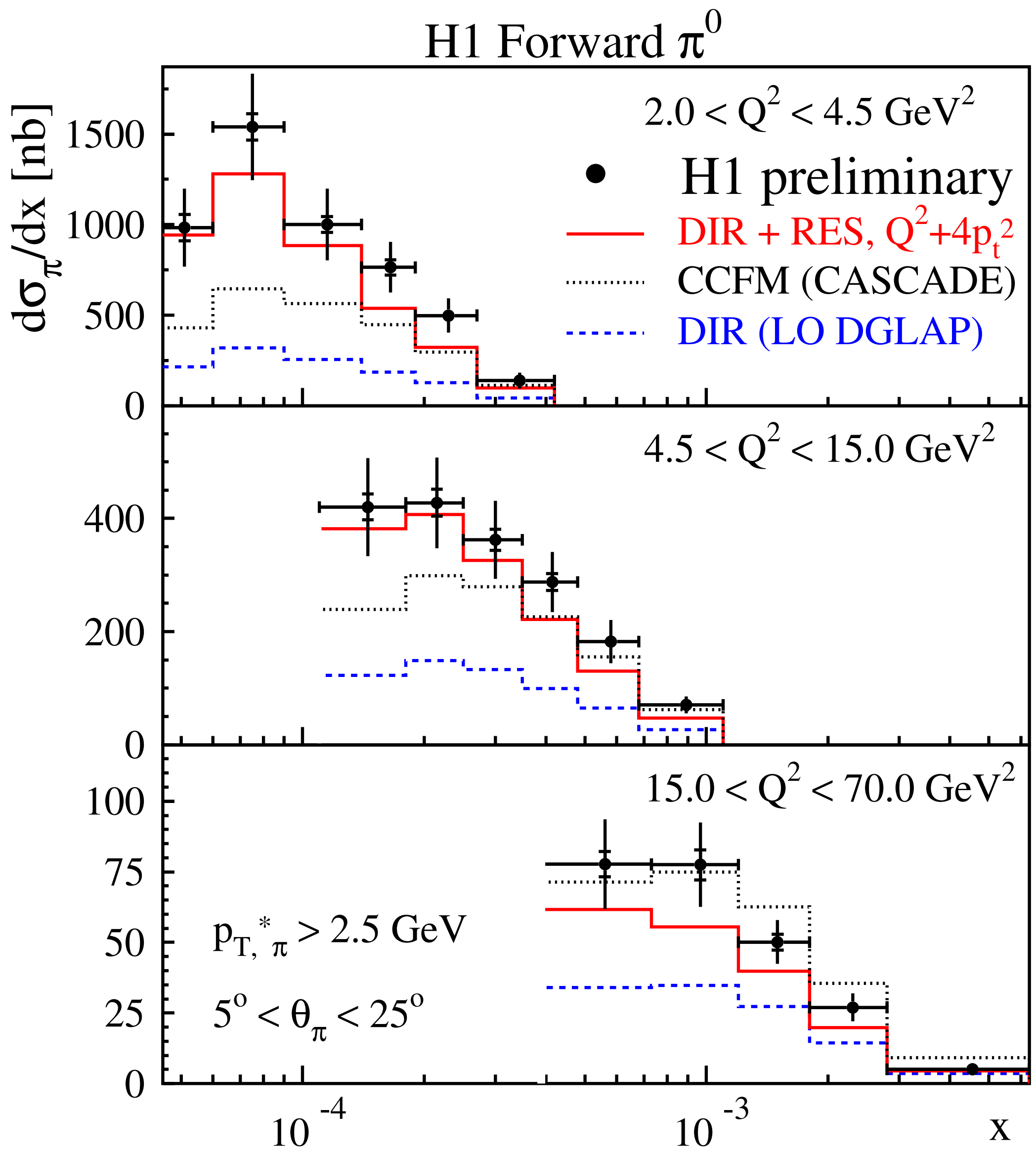

Figure 1: Inclusive π^0-meson production cross-sections as a function of Bjorken x for $p^*_{T,\pi} >$ 2.5 GeV in three regions of Q^2. The inner error bars are statistical, the outer error bars give the statistical and systematic error added quadratically. The QCD models RAPGAP based on LO DGLAP parton showers with (DIR+RES) and without (DIR) resolved photon processes and CASCADE, as an implementation of the CCFM equation, are compared to the data.

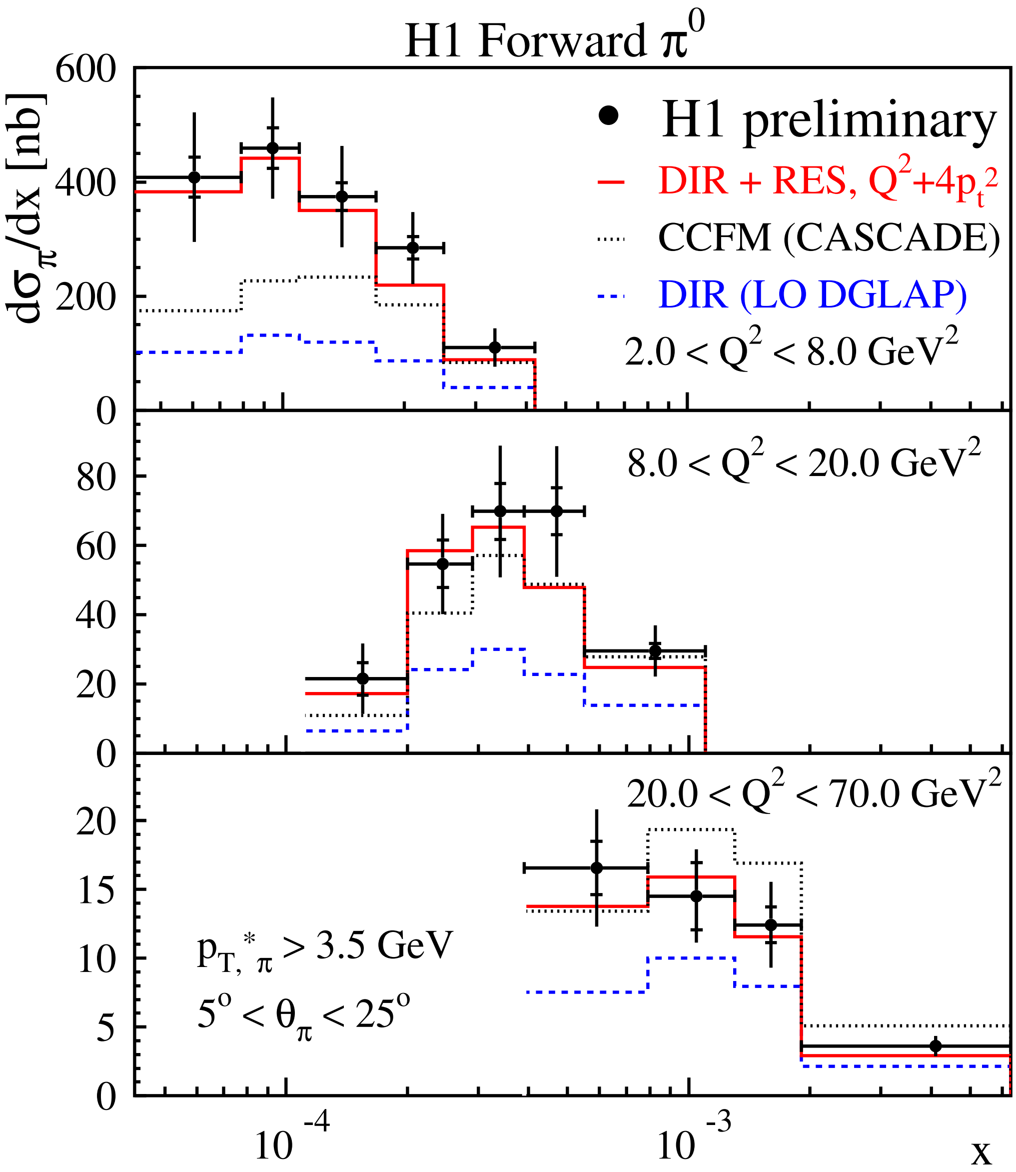

Figure 2: Inclusive π^0-meson production cross-sections as a function of Bjorken x for $p^*_{T,\pi} >$ 3.5 GeV in three regions of Q^2. The inner error bars are statistical, the outer error bars give the statistical and systematic error added quadratically. The QCD models RAPGAP based on LO DGLAP parton showers with (DIR+RES) and without (DIR) resolved photon processes and CASCADE, as an implementation of the CCFM equation, are compared to the data.

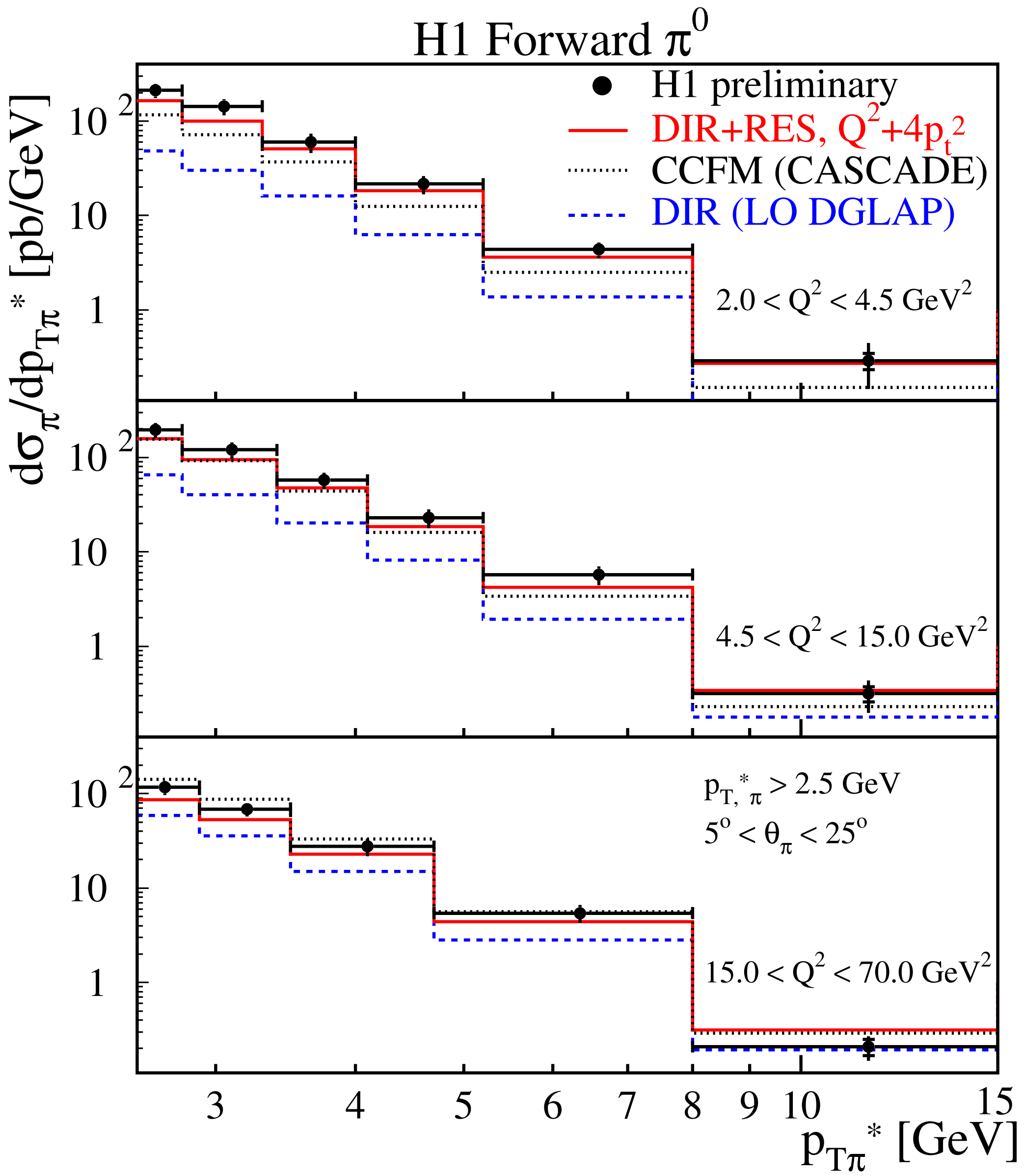

Figure 3: Inclusive π^0-meson production cross-sections as a function of $p^*_{T,\pi}$ for $p^*_{T,\pi}$ >2.5 GeV in three regions of Q^2. The inner error bars are statistical, the outer error bars give the statistical and systematic error added quadratically. The QCD models RAPGAP based on LO DGLAP parton showers with (DIR+RES) and without (DIR) resolved photon processes and CASCADE, as an implementation of the CCFM equation, are compared to the data.

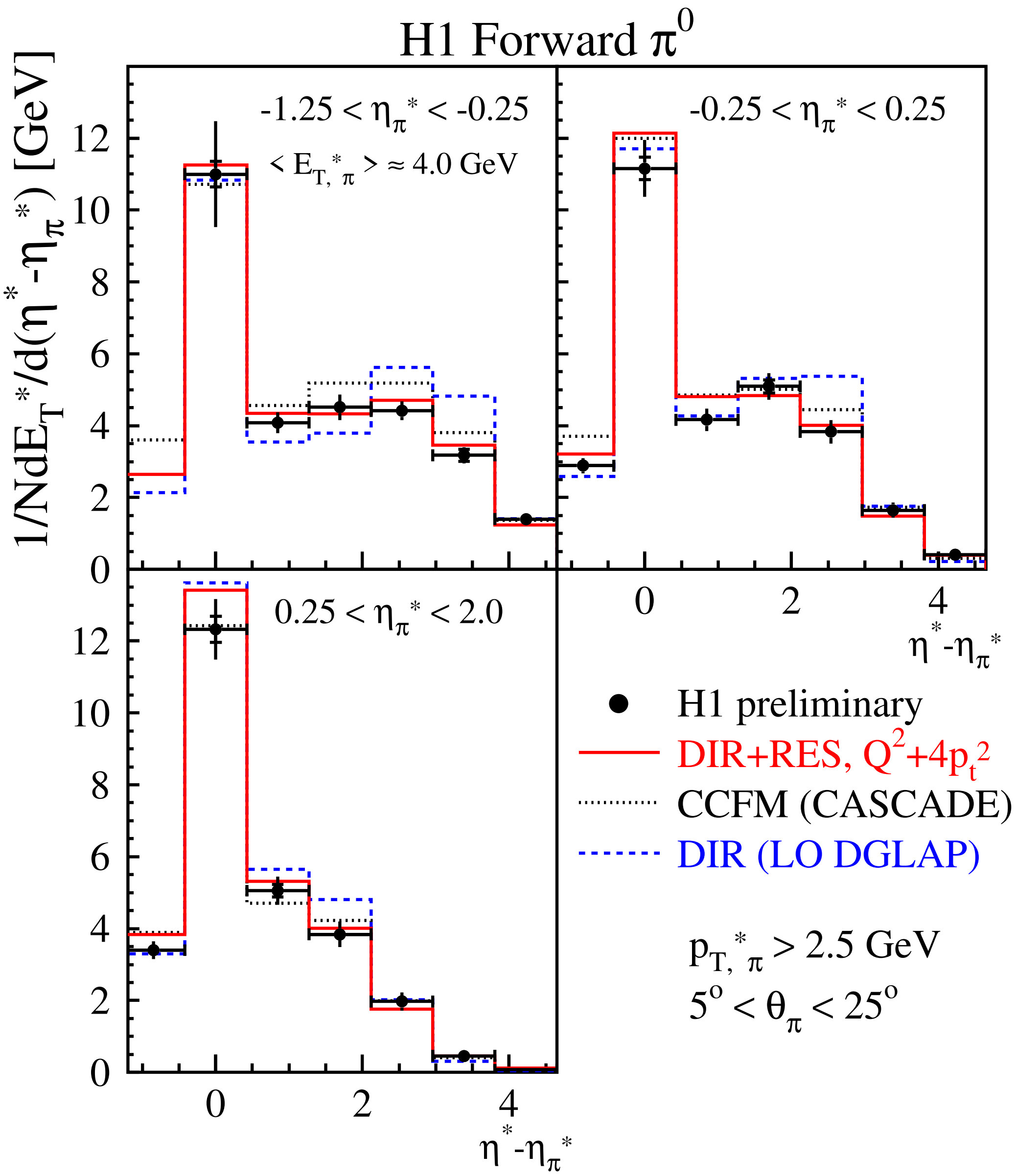

Figure 4: Transverse energy flow around the forward π^0 for different ranges of π^0 pseudorapidity dity η^*_π in the hadronic CMS as a function of the pseudorapidity distance from the π^0 direction. The incoming photon direction defines the $+z^*$ direction. The contribution from the forward π^0 is included in the distributions. The QCD models RAPGAP based on LO DGLAP parton showers with (DIR+RES) and without (DIR) resolved photon processes and CASCADE, as an implementation of the CCFM equation, are compared to the data.

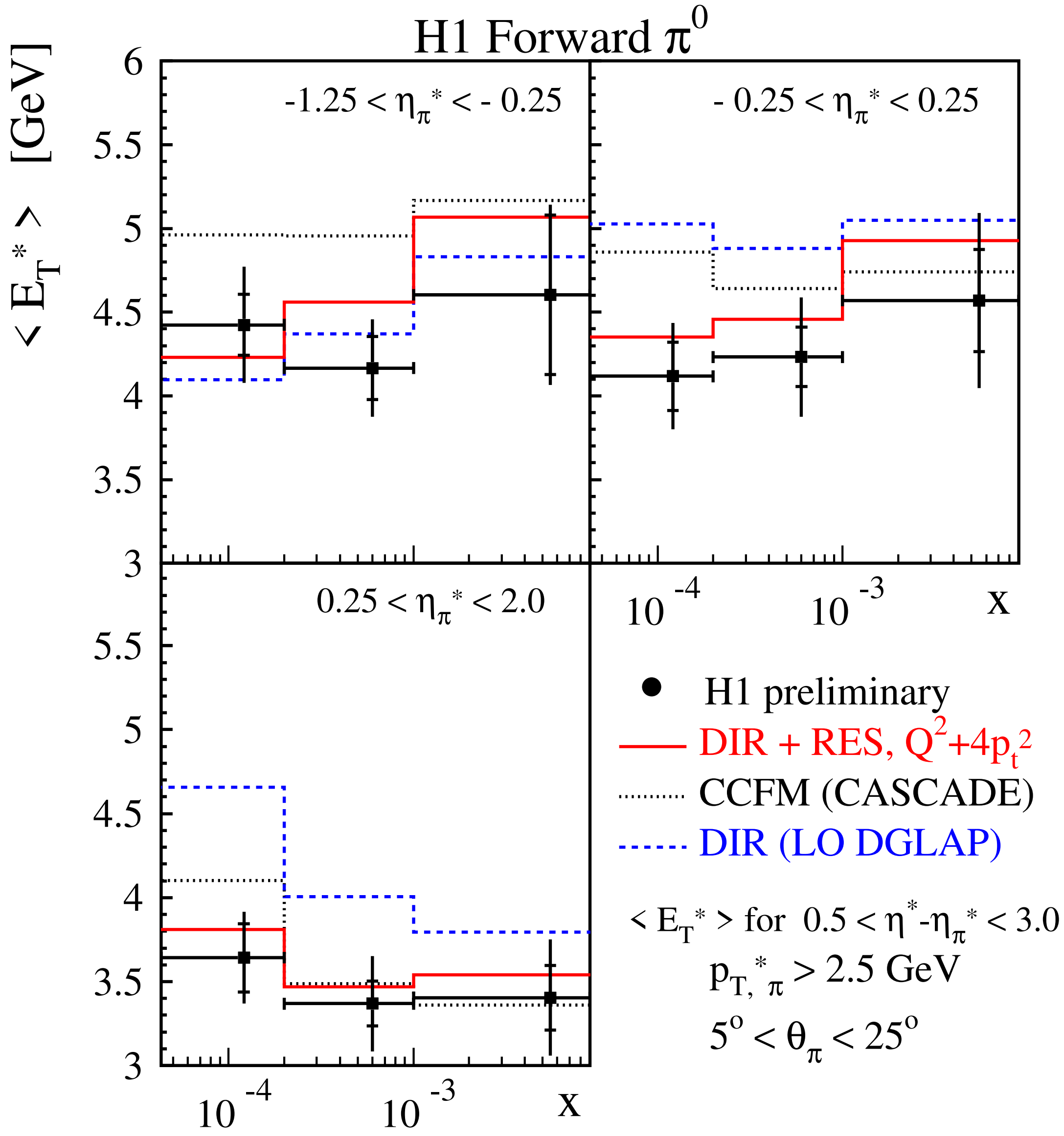

Figure 5: Mean transverse energy in the region $0.5 < \eta^* - \eta^*_\pi < 3.0$ for different ranges of η^*_π in the hadronic CMS as a function of Bjorken x. The QCD models RAPGAP based on LO DGLAP parton showers with (DIR+RES) and without (DIR) resolved photon processes and CASCADE, as an implementation of the CCFM equation, are compared to the data.